European Journal of Cardio-Thoracic Surgery 2023, 63(3), ezad040
https://doi.org/10.1093/ejcts/ezad040 Advance Access publication 6 February 2023

ORIGINAL ARTICLE

Cite this article as: Di Leonardo S, Vella D, Grillo CS, Martorana C, Torre S, Argano V *et al*. Hydrodynamic *ex vivo* analysis of valve-sparing techniques: assessment and comparison. Eur J Cardiothorac Surg 2023; doi:10.1093/ejcts/ezad040.

Hydrodynamic *ex vivo* analysis of valve-sparing techniques: assessment and comparison

Sofia Di Leonardo [a,†], Danila Vella [a,†], Carmelo Savio Grillo[b], Carla Martorana[b], Salvatore Torre [b,c], Vincenzo Argano[b,c] and Gaetano Burriesci [a,d,*]

[a] Bioengineering Group, Ri.MED Foundation, Palermo, Italy
[b] School of Medicine and Surgery, University of Palermo, Palermo, Italy
[c] Cardiac Surgery Unit, Policlinico Paolo Giaccone, University of Palermo, Palermo, Italy
[d] UCL Mechanical Engineering, University College London, London, UK

* Corresponding author. UCL Mechanical Engineering, Torrington Place, London WC1E7JE, UK. Tel: +44-020-76793922; e-mail: g.burriesci@ucl.ac.uk (G. Burriesci).

Received 6 September 2022; received in revised form 23 January 2023; accepted 3 February 2023

Key question

What is the impact of the valve-sparing procedure and graft configuration on the predicted aortic valve performance?

Key finding(s)

Dynamics and performance of the aortic root strongly depend on the graft configuration.

Take-home message

Grafts replicating Valsalva sinuses can restore more physiological valve dynamics and performances.

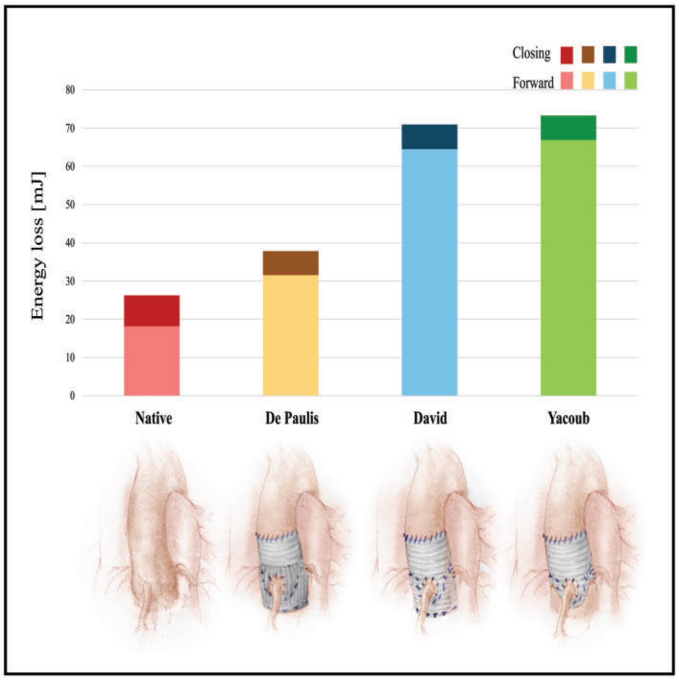

Abstract

OBJECTIVES: Valve-sparing procedures are surgical techniques allowing to restore adequate function of the native aortic valve by replacing the dysfunctional ascending aorta with a prosthetic conduit. A number of techniques are currently used, such as Yacoub's remodelling and David's reimplantation, based on a regular straight conduit. More recently, the De Paulis proposed the use of bulging conduits to reconstruct the shape of the Valsalva sinuses. This work investigates the impact of the valve-sparing technique on the aortic valve function.

†The first two authors contributed equally to this work.
Presented at the 36th EACTS Annual Meeting, Milan, Italy, 5-8 October 2022.

METHODS: The performance of 3 porcine aortic roots (Medtronic Freestyle^{TM}) was assessed in a cardiovascular pulse duplicator before and after performing 3 alternative valve-sparing procedures: David's reimplantation, Yacoub's remodelling and De Paulis' reimplantation.

RESULTS: The porcine aortic roots, representative of the healthy native configuration, were characterized by the highest efficiency, with a mean energetic dissipation under normal operating conditions of 26 mJ. David's and Yacoub's techniques resulted in significantly lower performance (with mean energetic loss of about 70 mJ for both cases). The De Paulis' procedure exhibited intermediate behaviour, with superior systolic performance and valve dynamics similar to the native case, and a mean energetic loss of 38 mJ.

CONCLUSIONS: The dynamics and performance after valve-sparing strongly depend on the adopted technique, with the use of conduits replicating the presence of Valsalva sinuses restoring more physiological conditions.

Keywords: Valve-sparing implants • Aortic root prosthesis • Hydrodynamic performance • *Ex vivo* analysis • Valsalva sinuses

ABBREVIATIONS

CO	Cardiac output
POA	Projected orifice area

INTRODUCTION

Despite its apparently simple anatomical morphology, the aortic root has the function to establish and maintain a haemocompatible intermittent laminar flow, proper coronary perfusion and optimum left ventricular function at the different operating conditions [1]. This involves a synergistic interplay between its different constituent elements at both, microscopic and macroscopic, levels. Dysfunctional pathologies such as aneurysms of the ascending aorta can alter these delicate mechanisms, resulting into major complications. In fact, abnormal dilation of the arterial vessel in proximity of the aortic valve can cause dislocation of the commissures, with consequent lack of coaptation of the valve leaflets, independently of their structural integrity. This may result in a clinical condition of aortic insufficiency, associated with reduced left ventricular function and ejection fraction, potentially leading to acute pulmonary oedema [2].

Aneurysmal pathology of the aortic root is normally treated through traditional surgical therapies, aimed at repairing the aortic root and resolve aortic insufficiency.

When the insufficiency has functional nature, and the native valve leaflets have maintained their integrity, their physiological function and anatomy can be restored by adopting common valve-sparing procedures [3], such as the David's 'reimplantation' technique [4] and the Yacoub's 'remodelling' technique [5]. In both approaches, the 3 sinuses of Valsalva are excised from the native root and replaced with a tubular straight graft. In particular, in David's procedure, the proximal edge of the graft is sutured at the annulus, whilst in the case of Yacoub's procedure, it is cut into a crown shape and sutured just above the leaflets attachment. Over the years, several reports have suggested that although Yacoub's remodelling procedure is physiologically superior to David's reimplantation procedure, with a more natural motion of the aortic annulus, it may be associated with higher risk of annulo-aortic ectasia and recurring insufficiency [6, 7]. David's technique, instead, provides a better stabilization of the aortic annulus, but the total removal of the Valsalva sinuses has been associated with suboptimal haemodynamics [8].

More recently, De Paulis *et al.* [9] proposed a re-adaptation of both techniques, replacing the tubular graft with a Gelweave Valsalva^{TM} (Vascutek, UK) graft, which incorporates a bulging segment that can replicate the presence of the Valsalva sinuses. In this case, the commissures of the native valve are stitched to the graft at the level of the suture between the bulging segment and the tubular portion of the prosthesis, acting as a sinotubular junction (STJ). Although the use of this graft is described for both, reimplantation and remodelling procedures, De Paulis *et al.* indicate it as particularly suitable to perfection the David's technique, as it could allow a more physiological leaflets dynamics, whilst stabilizing the annulus diameter.

Over the years, different studies investigated the performances of tubular and Valsalva conduits and the efficacy of reproducing Valsalva sinuses, finding discordant results [10, 11]. These results clearly expose that the optimal conduit for valve-sparing still needs to be identified [12], and the role of the Valsalva sinuses on the haemodynamics is far from being agreed upon.

This work presents an analysis and comparison of the hydrodynamic performance of the most common aortic root repair procedures, namely the David's reimplantation, Yacoub's remodelling and De Paulis' reimplantation, with the healthy native reference. The aim of this work is to assess the ability of each technique to restore healthy operating conditions by means of systematic *in vitro* testing, and verify if the attempt to restore the morphology of the Valsalva sinuses can provide a clinical advantage.

MATERIALS AND METHODS

Prosthesis implants

The Medtronic Freestyle^{TM} bioprosthetic aortic root was selected to represent healthy native operating conditions. This device consists of a porcine aortic root, cross-linked in dilute glutaraldehyde solution while applying 40 mmHg of internal pressure on the root (after ligating the coronary arteries at their inlet), to counteract shrinkage and maintain the natural commissural configuration. Leaflets undergo chemical fixation at zero differential pressure, thus minimizing changes in their flexibility and function. The valve inflow edge is covered with PET fabric, which extends over the ventricular muscle band present below the right coronary ostium, in order to strengthen this region (see Fig. 1) [13]. Despite some difference of proportion between the leaflets and the position in the coronary ostia, this prosthesis is recognized to closely emulate the healthy human aortic root in terms of anatomy and function [14]. Three prosthetic roots of size 25 mm (corresponding to the annulus diameter) were selected to represent healthy native conditions and tested in the pulse duplicator to assess their hydrodynamic performance. They were then used to perform 3 surgical valve-sparing techniques, and retested for each configuration. The surgical procedures were performed by

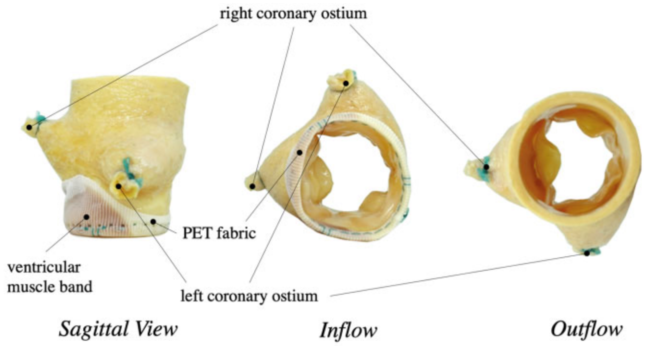

Figure 1: Freestyle prosthesis. Sagittal, inflow and outflow views.

the same experienced surgical team, in the following order: David's, Yacoub's and De Paulis'.

Before the implants, each graft was prepared by washing out the collagen coating and dipping the clean fabric in a silicone suspension (1-2577 Low VOC) to make it impermeable to the saline solution used as test fluid in the *in vitro* assessments. For the David's and Yacoub's techniques, a straight tubular graft made of surgical PET knitted fabric (Intergard) of 28 mm was used to achieve an increased sinuses diameter. David's reimplantation technique was performed by excising the Valsalva sinuses from the native root, just leaving few millimetres of aortic wall at the valve outflow. The proximal end of the tubular graft was sutured at the annulus, immediately below the aortic valve. The outflow edge was sutured to the graft wall (see Fig. 2). The Yacoub's configuration was directly derived from the David's, by removing the suture points at the aortic annulus and trimming a 3-pointed crown below the sutured line at the outflow edge. Subsequently, the graft was removed and the valve sutured into a Gelweave Valsalva™ conduit of 26 mm diameter, performing the reimplantation procedure as described by De Paulis *et al.* [9] (details about the surgical technique are reported in the Supplementary Material, S1).

All implants were fixed to a specifically designed 3D printed resin support, in order to minimize distortion during handling and allow easy and consistent positioning into the Pulse Duplicator for the hydrodynamic assessment (see Fig. 3).

In vitro testing

The hydrodynamic performance assessment of each implant was conducted *in vitro* on a hydro-mechanical pulse duplicator (ViVitro Superpump, SP3891, Canada). The system is composed of a servo controlled volumetric pump that allows the fluid circulation in 3 cardiac chambers separated by exchangeable heart valves. The fluid sections are equipped with an electromagnetic flowmeter (Carolina Medical, East Bend, North Carolina, USA) and pressure transducers (Utah Medical, Midvale, Utah, USA) placed in all cardiac cambers.

All roots were tested in the aortic position, following the order of the procedures (healthy native, David, Yacoub and De Paulis). A St Jude 29 mm bileaflet mechanical valve was used in the mitral position. In compliance with the *in vitro* test procedure of the ISO5840 standard [15], tests were carried out at 6 cardiac outputs (CO: 2, 3, 4, 5, 6 and 7 l/min), at a heart rate 70 bpm, with systolic

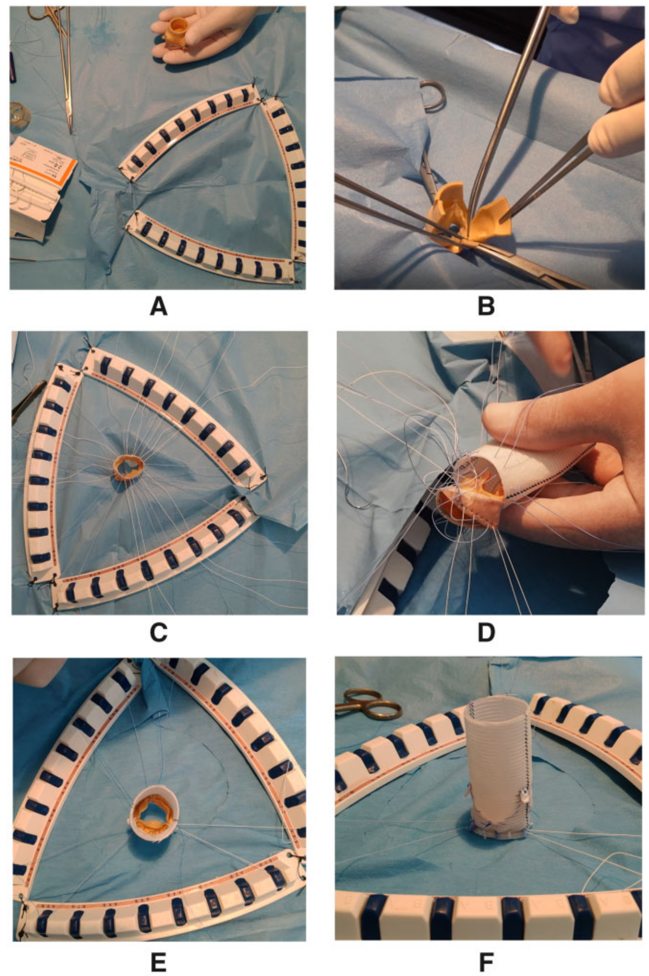

Figure 2: David implant steps: (**a**) equipment, (**b**) native valve cutting, (**c**) valve preparation, (**d**) graft suturing, final implant, (**e**) transversal and (**f**) sagittal views.

duration 35% and mean aortic pressure equal to 100 mmHg. Buffered saline solution at room temperature was used as test fluid. For each test, results were acquired over 10 consecutive cycles, reporting their mean and standard deviation.

The systolic performance was quantified on the basis of the mean systolic transvalvular pressure difference measured during the positive differential pressure period (ΔP), and of the effective orifice area (EOA), calculated based on the Gorlin's formula [16], as in Equation (1):

$$\mathrm{EOA} = \frac{Q_{vRMS}}{51.6\sqrt{\frac{\Delta P}{\rho}}}, \quad (1)$$

where Q_{vRMS} is the root mean square forward flow (mm/s), ρ is the density of the test fluid (g/ml) and ΔP is expressed in mmHg.

The diastolic performance was associated with the closing regurgitant volume, calculated as the integral of the flow curve during the closing valve period.

The global performance during the whole cardiac cycle was quantified on the basis of the left ventricular energy loss (E_{loss})

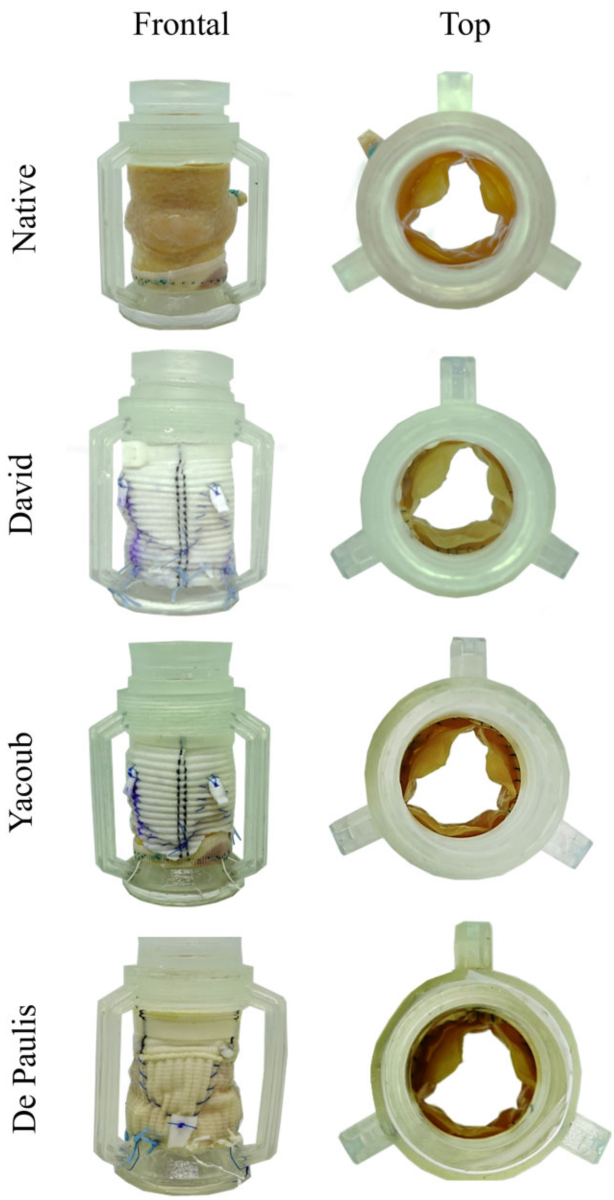

Figure 3: Healthy native prosthesis and valve-sparing implants, David, Yacoub and De Paulis, set into resin support.

[17, 18], calculated as the sum of the forward flow energy loss (E_{lossF}, measured during the ejection phase) and the closing energy loss (E_{lossC}, measured during the closing phase), determined in mJ from Equation (2) [19]:

$$E_{\text{loss}} = 0.1333 \int_{t_i}^{t_f} \Delta p \cdot q \cdot dt, \quad (2)$$

where t_i and t_f are the initial and final time instants of the phase where the energetic loss is quantified, Δp is the instantaneous transvalvular pressure (expressed in mmHg) and q is the instantaneous flow rate (expressed in mm/s).

High frame rate videos were recorded from the valve outflow at a CO of 5 l/min, to observe the valve dynamics in the different implants. These videos were binarized and analysed with a code specifically written in Matlab (MathWorks, USA) to quantify the instantaneous and mean projected orifice area (POA) [20].

Videos of the sagittal view were also analysed in Matlab to determine the variation of diameter occurring at the STJ during the cardiac cycle and compute the compliance as described in the ISO 5840 [15].

Statistical analysis

The performance parameters at CO of 5 l/min were analysed using an ANOVA test for repeated measures. Where a statistical difference was found, the Tukey's honestly significant difference test was used to perform the *post-hoc* pairwise comparison. A P-value < 0.05 was considered statistically significant. The size effect was estimated to evaluate the magnitude of the group differences, computing omega square (Ω^2). A $\Omega^2 > 0.14$ was considered as a large size effect [21].

RESULTS

Hydrodynamic performances

The performance parameters determined for each test are summarized in the diagrams in Fig. 4, where each column corresponds to a prosthesis.

For each valve, the ΔP indicates the best performance for the healthy native valve, with a mean value at 5 l/min of 4.49 mmHg, followed by the De Paulis' (mean of 6.45 mmHg). The David's and Yacoub's techniques resulted in similarly higher ΔP (mean of 9.07 and 8.76 mmHg, respectively), with the remodelling approach resulting slightly superior for valve 1 and slightly worse for the other 2 (see Fig. 4a–c). Globally, ΔP is statistically different among the groups ($P = 0.002$) with a large size effect ($\Omega^2 = 0.36$); however, the pairwise comparison does not result in any significant differences. The EOA reflects similar trends (Fig. 4d–f), resulting maximum for the 3 healthy native valves (with a mean value for all COs of 3.50 cm^2), followed by the De Paulis' (mean of 3.04 cm^2). The David's and Yacoub's (mean of 2.53 and 2.44 cm^2, respectively) mostly overlap at lower values. These differences are statistically significant, with $P < 0.001$ and a large size effect of $\Omega^2 = 0.63$. Moreover, the *post-hoc* comparison identifies significant differences in healthy native vs David ($P = 0.015$) and healthy native vs Yacoub ($P = 0.015$) (in Supplementary Material, Table S2.1, the details of Tukey's HSD *post-hoc* comparison are reported). The energetic contribution of the systolic phase (E_{lossF} in Fig. 5) is substantially lower for the healthy native configuration, followed by the De Paulis', which presents values more than 50% higher. For the David's and Yacoub's implants, these losses are about twice as for the De Paulis'.

All valves were fully competent in all configurations, with minimum leakage. The closing regurgitant volume has a variable trend (see Fig. 4g–i), with the David's implants characterized by more stable values among the tested COs (however difference is not statistically significant). In general, at high COs (≥ 5 l/min), the healthy native valve and Yacoub's (the 2 cases where the valve annulus is not constrained into the graft) appear to undergo larger closing regurgitant volume. The E_{lossC} results minimum for the De Paulis', intermediate for the David's and Yacoub's, and highest for the Freestyle (see Fig. 5). However, this loss has lower contribution compared to the systolic, and does not alter considerably the energetic efficiency of the different configurations. In fact, over the whole cycle, the E_{loss} (see Fig. 4l–n) confirms that

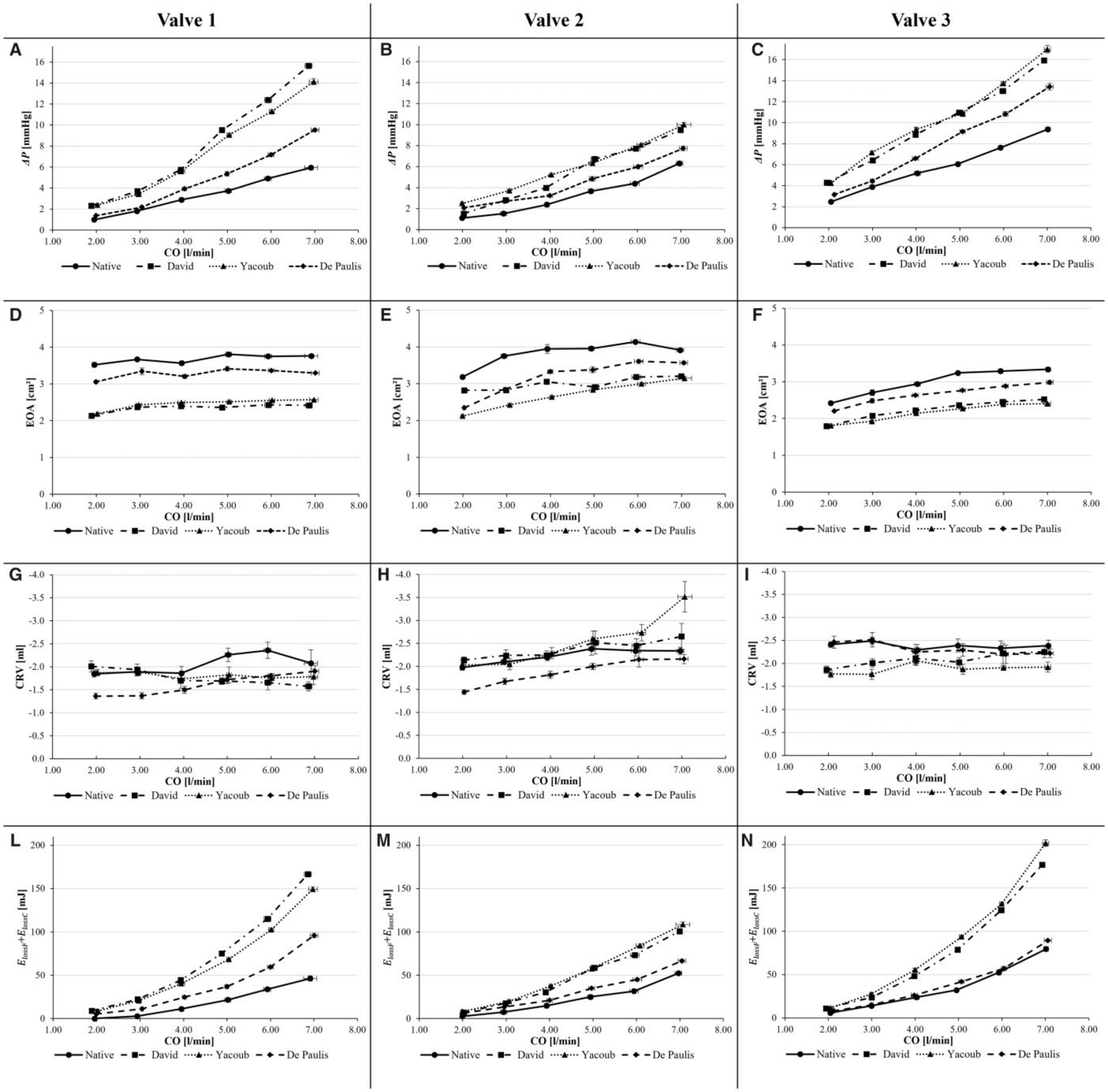

Figure 4: Implant performance parameter diagram of: (**a–c**) ΔP; (**d–f**) *EOA*; (**g–i**) *CRV*; (**l–n**) $E_{lossF} + E_{lossC}$. Each diagram reports mean performances value in 10 cycles. The standard deviation is reported as error bars.

the healthy native configuration is more efficient for all COs (with a mean value at 5 l/min of 26.24 mJ). The David's and Yacoub's are characterized by substantially higher E_{loss} (70.89 and 73.26 mJ, respectively), while the De Paulis' is much closer to the healthy native (37.84 mJ). The significance of the observed differences is confirmed by a $P < 0.001$ and a large size effect $\Omega^2 = 0.76$. The *post-hoc* comparison results in significant differences between all groups, but David vs Yacoub (see Supplementary Material, Table S2.1).

Table 1 summarizes the performance parameters obtained for all valves and configurations, at a standard CO of 5 l/min (in Supplementary Material, Table S3.2, performance parameters at all COs are reported).

High frame rate video analysis

The mean POA values indicate that the estimated EOA closely correspond to the geometric leaflets opening (see Fig. 6). Again, the healthy native valve exhibits the widest orifice area, with the De Paulis' implant associated with a decrease of POA of at least 10%, and the David's and Yacoub's implants with a reduction of

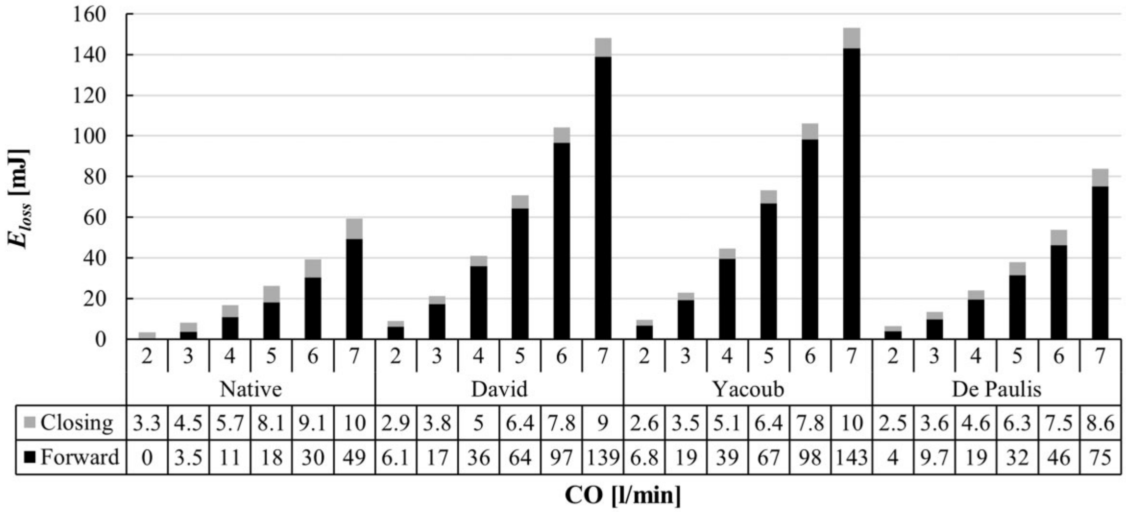

Figure 5: Mean E_{lossC} and E_{lossF} for each kind of implant.

Table 1: Implant performance parameter at 5 l/min of CO (distance from the healthy native result)

Valve	Configuration	ΔP (mmHg)	EOA (cm^2)	CRV (ml)	$E_{lossF} + E_{lossC}$ (mJ)
1	Native	3.74 SD: 0.12	3.81 SD: 0.07	−2.26 SD: 0.15	21.60 SD: 1.07
	David	9.53 SD: 0.25	2.36 SD: 0.02 (−38%)	−1.69 SD: 0.07	75.05 SD: 1.50
	Yacoub	9.07 SD: 0.14	2.52 SD: 0.03 (−34%)	−1.83 SD: 0.17	68.47 SD: 1.63
	De Paulis	5.36 SD: 0.19	3.41 SD: 0.06 (−10%)	−1.72 SD: 0.09	36.81 SD: 1.94
2	Native	3.66 SD: 0.10	3.96 SD: 0.05	−2.38 SD: 0.14	25.03 SD: 1.08
	David	6.73 SD: 0.07	2.91 SD: 0.01 (−27%)	−2.52 SD: 0.25	58.70 SD: 1.54
	Yacoub	6.32 SD: 0.09	2.84 SD: 0.02 (−28%)	−2.60 SD: 0.17	57.65 SD: 1.66
	De Paulis	4.84 SD: 0.23	3.38 SD: 0.08 (−15%)	−2.00 SD: 0.07	34.87 SD: 1.06
3	Native	6.06 SD: 0.13	3.24 SD: 0.04	−2.39 SD: 0.14	32.10 SD: 1.49
	David	10.97 SD: 0.20	2.36 SD: 0.02 (−25%)	−2.03 SD: 0.10	78.93 SD: 1.62
	Yacoub	10.88 SD: 0.29	2.27 SD: 0.03 (−28%)	−1.87 SD: 0.11	93.67 SD: 1.74
	De Paulis	9.15 SD: 0.13	2.76 SD: 0.02 (−12%)	−2.29 SD: 0.14	41.86 SD: 1.26

about 30% (healthy native > 3.16 cm^2; David = 2.20 cm^2, Yacoub = 2.25 cm^2 and De Paulis = 2.81 cm^2).

Regarding the measured compliance, the healthy native configuration displayed the highest value, equal to 11.5 %/100 mmHg. The David's implant had the smallest elasticity of 3.3 %/100 mmHg, whilst Yacoub's technique was effective in restoring some elasticity, increasing the compliance to 6.7 %/100 mmHg. The presence of corrugated sinuses in the De Paulis' provided an increased compliance of 7.9 %/100 mmHg; the largest after the native root.

DISCUSSION

All valves well exceeded the EOA requirements specified in the ISO 5840 standard [15], which for the size of 25 mm requires values ≥ 1.45 cm^2 at 5 l/min (all implants had a mean EOA > 2.54 cm^2). Still, despite the same implantation size, the 3 aortic roots exhibited some differences in the hydrodynamic behaviour. In particular, valve 2 appeared to be characterized by softer leaflets then the others, allowing wider opening and lower ΔP for all procedures. On the contrary, valve 3 resulted slightly more stenotic, with opening areas 15–20% smaller and ΔP about 60% higher than the other prostheses.

Nevertheless, the changes in performance parameters determined by each procedure were consistent for all 3 valves, confirming statistically significant trends.

As expected, the healthy native valves were characterized by the best efficiency. This appears to be driven by the superior physiological leaflets dynamics, with the leaflets expanding deep into the Valsalva sinuses to maximize the EOA, so as to minimize the ΔP and the associated E_{loss}. Analysis of the images in Fig. 6 shows that large portions of the leaflets expand further than the window of observation (this, represented as a red dashed line, has a diameter of 24 mm), with exception of the leaflet positioned at the bottom. This, for all valves, corresponds to the leaflet adjacent to the ventricular muscle band, stiffened by the presence of the PET fabric

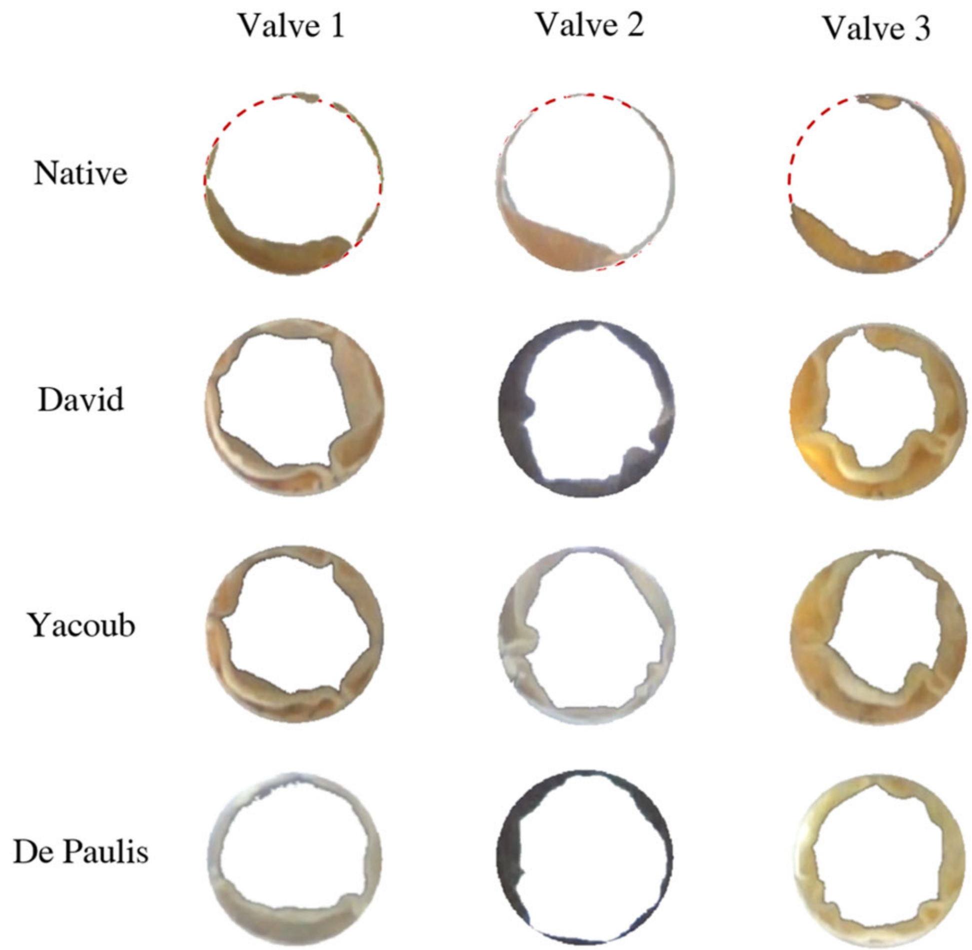

Figure 6: HFR images corresponding to the *POA* maximum value.

covering (represented in Fig. 1), which reduces the leaflet ability to expand into the right coronary sinus. The opening mechanism appears to be facilitated by the large compliance of the native aortic root, which undergoes relevant radial expansion during systole, increasing the EOA even further.

The use of a tubular graft in the David's and Yacoub's techniques, with consequent alteration of the sinus chambers, introduces a physical arrest to the valve leaflets which limits the achievable EOA. This levels the performance for the 2 approaches. The Yacoub's approach appears to double the compliance of the implant (3.3–6.7%), thanks to the 3-pointed crown at the leaflet attachment. Compared to the native root, the 2 techniques were characterized by a reduction of EOA and a major increase in ΔP (at a CO of 5 l/min, EOA was 25–38% lower and ΔP was 75–140% larger for the 3 valves). This is well reflected in the measurement of the POA, which shows a mean reduction of about 30% compared to the healthy native valve, easy to be visually appreciated in Fig. 6.

The attempt to replicate the presence of the Valsalva sinuses in the De Paulis' procedure appears effective in restoring a more physiological dynamics, with the leaflets allowed to expand into the more pronounced bulging section of the graft. The De Paulis' results in better systolic performance than the other 2 valve-sparing techniques, with an EOA reduced of just 10–15% compared to the healthy native configuration at a CO of 5 l/min (see Table 1). Again, this is well aligned with the results from the POA measurement.

Performing all sets of implants following the same sequence may introduce an order effect in the results. However, this option was preferred as it allows to minimize the valve manipulations due to the removal and re-suturing of the different grafts. In fact, adopting the selected sequence, only one suturing is requested for the David's and Yacoub's, and a second one for the De Paulis. Still, the configuration experiencing the largest number of manipulations, which is always the De Paulis, exhibits the best performance in all the 3 sparing procedures, proving that any bias introduced during manipulation is not substantial, nor sufficient to alter the order of the most favourable conditions.

In general, the wider leaflets expansion characterizing the healthy native root is accompanied by some larger closing backflow than the other solutions, except for valve 2, where the leaflets expand substantially also after all valve-sparing procedures. This is a crucial result, as it challenges the most commonly accepted theory in the literature, which regards the presence of the Valsalva sinuses as functional to generate and host the vortices facilitating the valve closing [22, 23]. Instead, the presented tests appear to confirm the mechanism recently proposed by Tango *et al.* [24] on the basis of a computational study of the idealized aortic root. This identifies the main role of the sinuses in supporting the systolic phase by providing a chamber where the leaflets can fully expand to reduce their interference with the ejected blood flow. In fact, as clearly displayed in Fig. 5, the E_{loss} typically associated with the systolic forward flow is far more relevant than that produced by the closing regurgitant flow.

Hence, optimizing the opening phase can offer massive advantages, which make tolerable some collateral, but minor, loss in the closing phase.

From a clinical perspective, the presented study indicates that the De Paulis' technique can result in better performance than the approaches based on tubular grafts, due to its ability to better reproduce the anatomy of the Valsalva sinuses and their contribution to a larger valve opening [10]. However, it needs to be observed that this result is inconsistent with a recent study reported by Paulsen *et al.* [11, 12]. This describes similar *in vitro* tests, but concludes that valve-sparing techniques based on the De Paulis' approach provide inferior performance than reimplantation procedures performed with straight tubular conduits. This appears to be associated with some major leakage measured with bulging grafts, possibly due to the implantation of the commissures below the sinotubular graft suture. This, in fact, may cause excessive radial dislocation of the valve commissures, causing some degree of infravalvular diastolic backflow (as in operating conditions typical of aneurysmal roots). Hence, although our findings indicate the De Paulis' technique as potentially superior, this outcome is necessarily procedural dependent, with the positioning of the commissures playing an essential role. In fact, as described, excessively low positioning of the valve may result in the insurgence of central leakage. On the contrary, excessively high positioning would obliterate the function of the sinuses, making them unable to provide adequate room to host the expanding leaflets. The presented study also reveals the potential role that *in vitro* tests may play in perfecting surgical techniques and supporting clinical training.

Limitations

The interpretation of the described findings shall take into consideration few approximations and limitations in the performed tests. The anatomy and mechanical properties of the glutaraldehyde-treated juvenile pig aortic root are expected to have some difference from the corresponding patient's component. Also, the saline solution used in the presented tests, and preferred to blood equivalents to prevent tissue changes that may affect the tissue properties between tests, has different physical properties from human blood.

Moreover, the reduction of David's and Yacoub's techniques performances compared to the healthy native configuration may be related with the inability of the procedure to generate anatomically ideal sinuses, and to the lower compliance of the fabric graft. The similarity between the David's and Yacoub's techniques may be justified by the utilization of a bio-root with a stiffened annulus, trigons and muscular ridge, as opposed to the human valve. This may reduce the compliance achievable in human with the Yacoub's procedure.

Although the adopted sample size provides statistically significant results in terms of differences between the alternative procedures (with large size effect), larger sizes might, in future tests, increase the confidence in the presented findings.

CONCLUSIONS

This work analyses and compares the hydrodynamic alterations introduced by the most common valve sparing procedures: David's reimplantation, Yacoub's remodelling and De Paulis' reimplantation.

The prostheses representative of the healthy aortic root expectedly resulted the most efficient, with maximum EOA, and minimum ΔP and E_{loss}. This shows that, despite providing generally good performance, current valve-sparing techniques are still suboptimal and far from matching the physiological leaflets dynamics. The significantly superior efficiency observed with the De Paulis' reimplantation technique confirms that replicating the anatomical features of the aortic root may contribute to enhance the efficacy of the treatment. Still, engineering improvement is needed to design conduits that better model the optimum compliance of the native vessel.

SUPPLEMENTARY MATERIAL

Supplementary material is available at *EJCTS* online.

Conflict of interest: none declared.

DATA AVAILABILITY

All relevant data are within the manuscript and its Supplementary data files. Further data underlying this article will be shared on reasonable request to the corresponding author.

Author contributions

Sofia Di Leonardo: Conceptualization; Data curation; Investigation; Validation; Visualization; Writing—original draft. **Danila Vella:** Conceptualization; Data curation; Investigation; Validation; Visualization; Writing—original draft. **Carmelo Savio Grillo:** Formal analysis; Investigation. **Carla Martorana:** Formal analysis; Investigation. **Salvatore Torre:** Conceptualization; Methodology; Supervision; Writing—review & editing. **Vincenzo Argano:** Conceptualization; Methodology; Resources; Supervision; Writing—review & editing. **Gaetano Burriesci:** Conceptualization; Data curation; Investigation; Project administration; Supervision; Validation; Visualization; Writing—original draft; Writing—review & editing.

Reviewer information

Reviewer information European Journal of Cardio-Thoracic Surgery thanks Giacomo Murana, Gabriele Piffaretti and the other, anonymous reviewer(s) for their contribution to the peer review process of this article.

REFERENCES

[1] Sievers H-H, Hemmer W, Beyersdorf F, Moritz A, Moosdorf R, Lichtenberg A *et al.*; Working Group for Aortic Valve Surgery of German Society of Thoracic and Cardiovascular Surgery. The everyday used nomenclature of the aortic root components: the tower of Babel? Eur J Cardio-Thoracic Surg 2012;41:478–82.
[2] Salameh MJ, Black JH, Ratchford EV. Thoracic aortic aneurysm. Vasc Med 2018;23:573–8.
[3] David TE. Aortic valve sparing in different aortic valve and aortic root conditions. J Am Coll Cardiol 2016;68:654–64.
[4] David TE, Feindel CM. An aortic valve-sparing operation for patients with aortic incompetence and aneurysm of the ascending aorta. J Thorac Cardiovasc Surg 1992;103:617–21; discussion 622.
[5] Sarsam MAI, Yacoub M. Remodeling of the aortic valve anulus. J Thorac Cardiovasc Surg 1993;105:435–8.
[6] Maskell P, Brimfield M, Ahmed A, Harky A. In patients undergoing valve-sparing aortic root replacement, is reimplantation superior to remodelling? Interact Cardiovasc Thorac Surg 2021;32:441–6.

[7] Kunihara T. Valve-sparing aortic root surgery. CON: remodeling. Gen Thorac Cardiovasc Surg 2019;67:82–92.
[8] Beckmann E, Leone A, Martens A, Mariani C, Krueger H, Cebotari S *et al.* Comparison of two strategies for aortic valve-sparing root replacement. Ann Thorac Surg 2020;109:505–11.
[9] De Paulis R, De Matteis GM, Nardi P, Scaffa R, Colella DF, Chiarello L. A new aortic Dacron conduit for surgical treatment of aortic root pathology. Ital Heart J 2000;1:457–63.
[10] Pisani G, Scaffa R, Ieropoli O, Dell'Amico EM, Maselli D, Morbiducci U *et al.* Role of the sinuses of Valsalva on the opening of the aortic valve. J Thorac Cardiovasc Surg 2013;145:999–1003.
[11] Paulsen MJ, Imbrie-Moore AM, Baiocchi M, Wang H, Hironaka CE, Lucian HJ *et al.* Comprehensive ex vivo comparison of 5 clinically used conduit configurations for valve-sparing aortic root replacement using a 3-dimensional-printed heart simulator. Circulation 2020;142:1361–73.
[12] Paulsen MJ, Kasinpila P, Imbrie-Moore AM, Wang H, Hironaka CE, Koyano TK *et al.* Modeling conduit choice for valve-sparing aortic root replacement on biomechanics with a 3-dimensional-printed heart simulator. J Thorac Cardiovasc Surg 2019;158:392–403.
[13] Sintek CF, Fletcher AD, Khonsari S. Stentless porcine aortic root: valve of choice for the elderly patient with small aortic root? J Thorac Cardiovasc Surg 1995;109:871–6; discussion 876.
[14] Kincaid EH, Kon ND. Freestanding root technique for implantation of the stentless Medtronic Freestyle valve. Oper Tech Thorac Cardiovasc Surg 2006;11:166–72.
[15] ISO 5840-1:2021 (E) Cardiovascular Implants Cardiac Valve Prosthes — Part 1: General requirements. International Organization for Standardization, Geneva, Switzerland.
[16] Garcia D, Kadem L. What do you mean by aortic valve area: geometric orifice area, effective orifice area, or Gorlin area? J Heart Valve Dis 2006; 15:601–8.
[17] Toninato R, Salmon J, Susin FM, Ducci A, Burriesci G. Physiological vortices in the sinuses of Valsalva: an *in vitro* approach for bio-prosthetic valves. J Biomech 2016;49:2635–43.
[18] Akins CW, Travis B, Yoganathan AP. Energy loss for evaluating heart valve performance. J Thorac Cardiovasc Surg 2008;136:820–33.
[19] Tango AM, Ducci A, Burriesci G. In silico study of the ageing effect upon aortic valves. J Fluids Struct 2021;103:103258.
[20] Susin FM. Complete unsteady one-dimensional model of the net aortic pressure drop. Open Biomed Eng J 2019;13:83–93.
[21] Serdar CC, Cihan M, Yücel D, Serdar MA. Sample size, power and effect size revisited: simplified and practical approaches in pre-clinical, clinical and laboratory studies. Biochem Med (Zagreb) 2021;31:27–53.
[22] Bellhouse BJ, Talbot L. The fluid mechanics of the aortic valve. J Fluid Mech 1969;35:721–35.
[23] Bellhouse BJ, Bellhouse FH, Reid KG. Fluid mechanics of the aortic root with application to coronary flow. Nature 1968;219:1059–61.
[24] Tango AM, Salmonsmith J, Ducci A, Burriesci G. Validation and extension of a fluid–structure interaction model of the healthy aortic valve. Cardiovasc Eng Technol 2018;9:739–51.